https://doi.org/10.1595/205651324X16964134291592 *Johnson Matthey Technol. Rev.*, 2024, **68**, (3), 307–321

JOHNSON MATTHEY
TECHNOLOGY REVIEW

technology.matthey.com

Inelastic Neutron Scattering Studies of Propene and 1-Octene Oligomerisation in H-ZSM-5

Increasing alkene yields *via* more selective zeolite catalysis

Alexander P. Hawkins
Central Laser Facility, Science and Technology Facilities Council, Research Complex at Harwell, Rutherford Appleton Laboratory, Harwell, OX11 0QX, UK

Andrea Zachariou
Department of Chemistry, Durham University, South Road, Durham, DH1 3LE, UK

Paul Collier
Johnson Matthey, Blounts Court, Sonning Common, Reading, RG4 9NH, UK

Russell F. Howe
Department of Chemistry, University of Aberdeen, Aberdeen, AB24 3UE, UK

David Lennon
School of Chemistry, University of Glasgow, Joseph Black Building, Glasgow, G12 8QQ, UK

Stewart F. Parker*
ISIS Neutron and Muon Source, STFC Rutherford Appleton Laboratory, Chilton, Oxon, OX11 0QX, UK

***Email:** stewart.parker@stfc.ac.uk

PEER REVIEWED

Received 7th September 2023; Accepted 4th October 2023; Online 4th October 2023

Neutron scattering methods such as quasielastic neutron scattering (QENS) and inelastic neutron scattering (INS) have been used to study the reactivity of propene and 1-octene over the acid zeolite catalyst H-ZSM-5. The high activity of the catalyst causes the alkenes to form linear oligomers below room temperature. INS has shown that the reaction proceeds through a hydrogen-bonded intermediate. Studies using propane as an inert analogue for propene have found that the adsorbed C3 molecules spend much of their time undergoing short jumps within the pore channels of the zeolite. Hydrothermal dealumination plays an important role in determining the activity of zeolite catalysts. Dealumination was found to delay the onset of catalytic activity for oligomerisation to higher temperatures and increase the mobility of hydrocarbons within the zeolite, both due to reduced acid-hydrocarbon interactions.

1. Introduction

ZSM-5 is an MFI-type zeolite that does not occur naturally and was developed by Mobil in the 1960s (1). It is typically synthesised using a tetrapropylammonium ion as a template. The crystal structure of ZSM-5 has been comprehensively investigated: there are over 100 reports in the International Zeolite Association database (2). The structure is based on 10-member ring windows that form a system of intersecting pores normal to each other, which are straight in the [010] direction and sinusoidal in the [100] direction. The pores are elliptical, having dimensions of 5.3 × 5.6 Å in the

© 2024 Johnson Matthey

straight channels and 5.1 × 5.5 Å in the sinusoidal channels.

ZSM-5 is a conventional aluminosilicate zeolite but is notable in that its stable range of Si:Al ratios is considerably higher than for other framework structures, ranging from 12:1 all the way up to effectively infinity in silicalite. Ratios <12:1 are typical for zeolites based on faujasite and chabazite frameworks.

In the acid form, H-ZSM-5, it has widespread commercial use as an additive catalyst in fluidised catalytic cracking (FCC) units, which are used to convert heavy petrochemical fractions such as vacuum gasoil to more profitable fractions such as gasoline and light alkenes (3). In FCC use, solid acid zeolites protonate hydrocarbon reactants to carbocations, enabling subsequent isomerisation or bond cleavage reactions to generate shorter chain or more highly branched hydrocarbons, which have greater commercial value. In such reactions, the aromatic or alkenic components of the reactant feed are the most actively converted by the zeolite, due to being easier to protonate. Saturated paraffins may be cracked or isomerised but this requires the use of zeolites with high levels of acidity. Industrial cracking units use a fluidised bed or regeneration system in order to deal with the carbonaceous 'coke' species that build up on the zeolite during use and which reduce its activity through pore blocking. The catalyst is continually cycled between the reactor and a separate regenerator unit where the coke is oxidised before being returned for re-use; allowing continual operation of the reactor despite coke buildup.

Current interest in H-ZSM-5 principally arises from its ability to increase the production of light alkenes (alkenes in the C_2–C_5 size range) and particularly propene as part of the FCC. These are valuable hydrocarbon products, both due to demand from the polymers industry and their use as feedstock chemicals for a wide range of chemical processes including production of acrylic acid, cumene and acrylonitrile. Historically the majority of global propene production has been as a byproduct of the steam cracking of light alkane fractions to produce ethene. However, while the market for propene continues to increase, global production lags behind demand by an increasing margin. Commercial steam cracking units are increasingly shifting to input streams from shale gas sources and are also improving in overall conversion efficiency, resulting in decreased output of products other than their target ethene. Increasing alkene yields from the FCC cracking of gasoline *via* more selective catalysis is an area of current industrial interest, with H-ZSM-5 being the main zeolite used in this application.

In this review, we describe recent work (4–8) on the interactions of propene and 1-octene (this is used as a model feedstock) with H-ZSM-5. In particular, we highlight the major effect that dealumination has on the chemistry. We use QENS and INS to study the mobility and local environment of the molecules in the zeolite.

2. Neutron Scattering

In addition to conventional methods such as surface area measurements, ammonia chemisorption, nuclear magnetic resonance, powder X-ray diffraction, we have extensively used QENS and INS to study the mobility and local environment of the molecules in the zeolite. As these are less commonly used techniques, we provide a brief introduction to them here. More detailed descriptions of neutron scattering (9), QENS (10) and INS (11) are available. Neutron studies of catalysts and catalytic processes have been reviewed recently (12–14).

While neutrons are very common, ~50% of terrestrial matter are neutrons, they are very strongly bound in atomic nuclei. The only current techniques that provide sufficient flux for use in condensed matter studies are nuclear fission and spallation. The former uses fission of ^{235}U to produce a self-sustaining nuclear reaction to provide neutrons for research. The latter uses a high energy proton beam that impacts a heavy metal (tantalum, tungsten, mercury) target. This produces highly excited nuclear states that 'evaporate' neutrons.

Newly born neutrons have energies in the several MeV range, these are brought to useful energies (a few meV to 500 meV, i.e. a few cm^{-1} to 4000 cm^{-1}, 1 meV = 8.066 cm^{-1}) by multiple inelastic collisions with a hydrogenous material ('moderation'). Reactors and spallation sources differ in the extent of moderation, so are complementary sources. Reactors are heavily moderated so the peak flux is around 25 meV, with no high energy neutrons, while spallation sources are deliberately under-moderated, so as to preserve the high energy neutrons and provide a full spectral range, 0–500 meV (0–4034 cm^{-1}), of neutrons.

The usefulness of neutrons arises from their properties. The neutron has a mass of ~1 atomic mass unit, it is uncharged, but it is a spin ½ particle. Neutrons, because they are uncharged,

 © 2024 Johnson Matthey

are scattered by atomic nuclei *via* the strong force. As the nucleus of an atom is only approximately one hundred thousandth the diameter of the atom, this means that most of matter is empty space to a neutron and neutrons are highly penetrating. A centimetre or so of steel is essentially transparent to a neutron. The mass means that in any scattering event, the neutron exchanges momentum (Q, Å^{-1}) with the scattering atom (i.e. there is a change of direction of the neutron). The scattering can be elastic, where there is no energy transfer between the neutron and the scattering atom, ($\Delta E = 0$), or inelastic, where energy exchange occurs ($\Delta E \neq 0$) ΔE can be positive (neutron energy gain) or negative (neutron energy loss). Elastic scattering provides information on the location of atoms (neutron diffraction is the most familiar example). Inelastic scattering provides information on their dynamics. This spans a range of energy transfers from almost zero (hence QENS), which gives access to diffusion constants at the atomic level, to the equivalent of the infrared region which provides vibrational spectra of materials (INS). While both techniques are applicable to all atoms, in practice, the large scattering cross section of ^{1}H (82 barn, 1 barn = 10^{-28} m^2, most other elements are 5 barn or less) means that if hydrogen is present in the material, then the scattering by hydrogen dominates. For QENS this means that single particle diffusion is observed. For INS, this means that the entire mid-infrared spectral region is available. In contrast, in the infrared spectrum, zeolites show intense lattice mode absorptions, which means that the spectra are restricted to the approximately 1800–4000 cm^{-1} range (in diffuse reflectance infrared Fourier transform spectroscopy) and approximately 1400–4000 cm^{-1} in transmission and the diagnostic 'fingerprint region' (400–2000 cm^{-1}) is largely inaccessible.

3. Discussion

In this section we will show how neutron scattering methods can help understand the chemistry of FCC processes. We will only discuss the results from neutron scattering, but it is important to emphasise that these are only part of the work that includes microreactor studies as well as a comprehensive characterisation of the catalyst supplied by Johnson Matthey (15). A related programme of work has featured the methanol-to-hydrocarbons reaction (16).

3.1 1-Octene

1-Octene is commonly used as a model compound for the cracking of long-chain alkenes to propene in FCC processes (17). The H-ZSM-5 catalyst (supplied by Johnson Matthey) has a lattice Si:Al ratio of 20 ± 5:1, with 3.26 Brønsted sites, 1.11 extra-framework aluminium hydroxyls and 0.66 silanols per unit cell (15). Introduction of 1-octene vapour into the fresh catalyst (ZSM-5-FR) results in the spectra shown in **Figure 1** (4). The spectra were

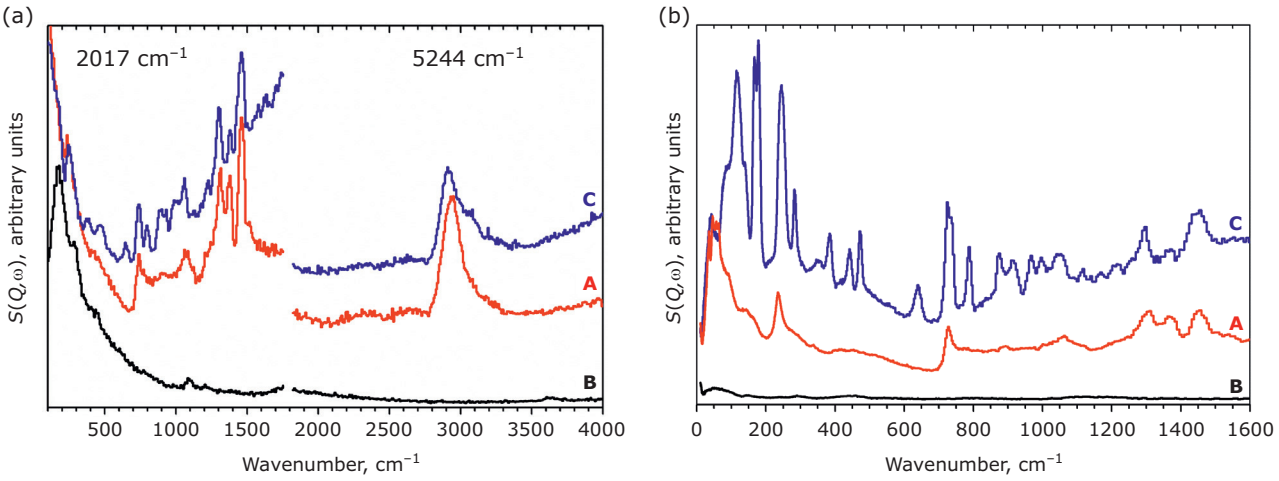

Fig. 1. (a) MAPS INS spectrum of 1-octene: A = following adsorption in ZSM-5-FR at room temperature; B = compared with the spectra of the ZSM-5-FR only; C = compared with pure 1-octene. Spectra recorded at incident energies of 2017 cm^{-1} and 5244 cm^{-1} and integrated over the momentum transfer range $0 \leq Q \leq 10$ Å^{-1}; (b) TOSCA INS spectra of: A = 1-octene in ZSM-5-FR; B = ZSM-5-FR; and C = pure 1-octene. The intensities have been scaled to correct for the different zeolite sample sizes and are offset for clarity. Reproduced from (4) with permission of the American Chemical Society

© 2024 Johnson Matthey

collected with two different INS instruments, MAPS **(Figure 1(a)**) and TOSCA **(Figure 1(b)**), at the ISIS Neutron and Muon Source (18). As explained elsewhere (11, 19), the instruments operate in different fashions, however, for the present work, the key difference is that MAPS provides access to the region >2000 cm^{-1}, hence can observe the C–H and O–H stretch region, while TOSCA is optimal in the 0–2000 cm^{-1} region, thus the instruments are highly complementary.

In **Figure 1**, Curves A and B, the spectra are normalised to the same quantity of zeolite. It can be seen that the scattering from the empty zeolite (**Figure 1**, Curve B) is negligible. This is a consequence of the small number of hydroxyls present and the small scattering cross-sections of oxygen, aluminium and silicon. Comparison of the spectra of the adsorbed species, **Figure 1**, Curve A with that of reference spectra of 1–octene, **Figure 1**, Curve C, shows little similarity. In particular, the alkenic sp^2 C–H stretch modes above 3000 cm^{-1}, the (C=C) torsion at 639 cm^{-1}, the intense transverse acoustic modes at 167 cm^{-1} and 178 cm^{-1} have all disappeared. It is clear that the 1-octene has undergone a reaction on adsorption into H-ZSM-5 at room temperature. Comparison with reference spectra of long-chain *n*-alkanes and polyethylene (21) suggests that the reaction has produced a mixture of multiple straight chain lengths, with no evidence of branching.

Zeolites are well-known to cause oligomerisation of short chain alkenes (20). The literature indicates that eight-carbon molecules, for example, 1-octene, are stable species in ZSM-5 at room temperature and while protonation occurs, the resulting carbocations are unreactive (22). This is not the case here.

The mobility of the 1-octene oligomers was investigated by QENS on the instrument IRIS at the ISIS facility. As a reference, we have first studied pure 1-octene and the results are shown in **Figure 2**. An elastic fixed window scan (EFWS) was recorded at 10 K intervals from 10 K to 370 K, with high signal-to-noise ratio (SNR) spectra being recorded at 5 K (for the resolution function where everything is immobile) and 220 K, 270 K, 320 K and 370 K in the liquid phase of 1-octene. The elastic intensity at a given temperature is inversely proportional to sample mobility. Mobility is initially minimal and increases only slowly while the sample remains in the solid state. On exceeding its melting point (171.5 K) the 1-octene undergoes a rapid increase in mobility as it enters the liquid phase and the elastic intensity drops to essentially zero by *ca*. 270 K, indicating that almost the entire sample is undergoing motion at this temperature.

An example of the analysis of the high SNR spectra is shown in the middle part of **Figure 2** for the 220 K data. This consists of the convolution of the resolution function (the data recorded at 5 K) with a Lorentzian line and a flat background. The latter accounts for motions that are too fast to be observed on this spectrometer. It can be seen that the full width at half maximum of the Lorentzian component (Γ, meV) increases as the momentum transfer (Q, $Å^{-1}$) increases. Plotting Γ *vs*. Q^2 produces the plot shown in **Figure 2(c)**. The dependence of Γ on Q^2 is specific to the mechanism of the translational motion (11). Fickian diffusion shows a linear relationship between Γ and Q^2 as shown in the 270 K, 320 K and 370 K data (**Figure 2**, Curves B, C and D respectively). At the lowest temperature 220 K, Curve A, the low Q plot is linear (from which the diffusion constant can be extracted), at high Q the data deviates from the linear relationship, showing that jump diffusion also occurs.

When the measurements are repeated for ZSM-5-FR and 1-octene loaded ZSM-5-FR, the EFWSs are shown in **Figure 3(a)**. These measurements were performed on the OSIRIS instrument, which for these purposes has almost identical performance to IRIS. It can be seen that the EFWS for ZSM-5-FR **Figure 3(a)**, Curve A is essentially flat, showing that there is little or no motion occurring, consistent with a rigid structure. Addition of 1-octene results in a large increase in intensity because of the large cross section of ^1H. It also confirms that the oligomerisation reaction has proceeded to completion during the room temperature dosing process; the rate of intensity change with temperature is nearly constant across the temperature range without any phase transitions as were observed for the 1-octene (**Figure 2(a)**) and the overall increase in mobility is much smaller than that observed for the free 1-octene.

Analysis of the data shows that even for the highest temperature investigated (373 K), the resolution function remains the major component of the overall scattering function across the entire Q range. This is in sharp contrast to the comparable results for the free 1-octene in **Figure 2** and indicates that even at this high temperature the majority of the hydrocarbon in the sample remains immobile.

The Lorentzian function was found to only significantly contribute to the overall scattering

 © 2024 Johnson Matthey

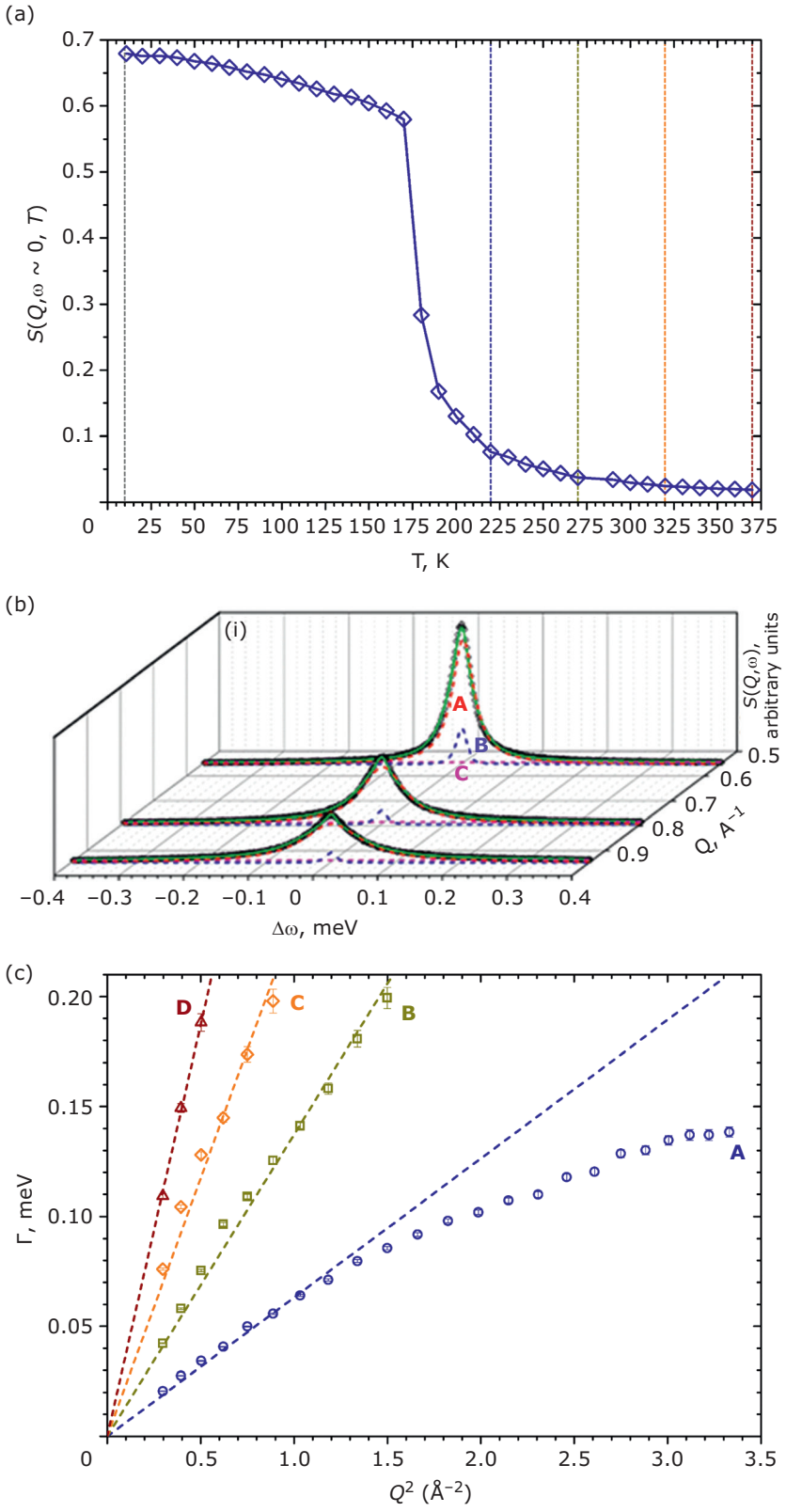

Fig. 2. (a) Elastic fixed window scan data for 1-octene from 10 to 370 K recorded on IRIS. Temperatures where high resolution data was collected for additional analysis are highlighted; (b) *S*(Q, ω) functions at selected values of Q for 1-octene at 220 K showing deconvolution into: A = resolution function, B = Lorentzian and C = linear background contributions; (c) variation of Lorentzian linewidth (Γ) as a function of Q^2 for the self-diffusion of 1-octene at: A = 220 K; B = 270 K; C = 320 K and D = 370 K. Dotted lines show the best fit of the data to Fickian diffusion

© 2024 Johnson Matthey

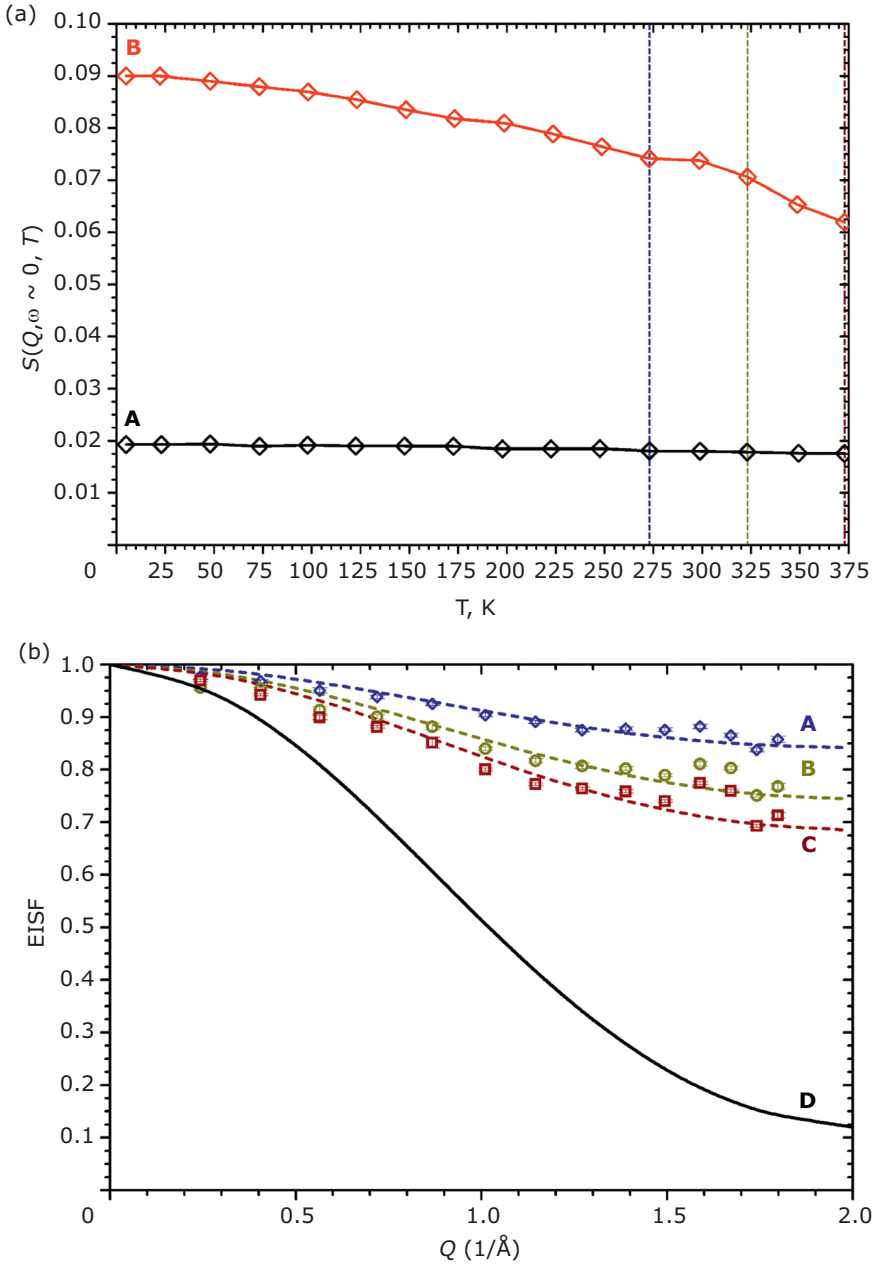

Fig. 3. (a) Elastic fixed window scan data for: A = ZSM-5-FR; B = 1-octene adsorbed in ZSM-5-FR from 5 K to 373 K recorded on OSIRIS. Temperatures where high SNR data was collected for additional analysis are highlighted; (b) the experimental EISF values of: A = 1-octene in ZSM-5-FR at 273 K; B = 323 K; C = 373 K are compared with the calculated EISF expected from continuous uniaxial rotation of the alkyl chain; D = assuming all the hydrogen atoms participate. The dotted lines show the results of inclusion of a partially-immobile fraction of hydrogens. Adapted from (4) with permission of the American Chemical Society

function at higher Q values: as was also found for the spectra at 273 K and 323 K. Since Q and distance are inversely related, this indicates that the hydrocarbon is limited to localised motion and it does not exhibit the long-range transport reported for linear alkanes in ZSM-5. Hence the oligomerisation reaction has resulted in a product which is sufficiently large to be immobilised (on the tens of picoseconds timescale of the QENS spectrometer (OSIRIS) used here) within the pore structure of the zeolite by interactions with the pore walls and with only a limited range of possible movement.

Localised motions in a QENS spectrum may be categorised by deriving the elastic incoherent structure factor (EISF, $A_0(Q)$) which is the fraction of the total scattering intensity that is elastic. Since the hydrocarbon is a long alkyl chain that

 © 2024 Johnson Matthey

is contained within pores whose diameter is less than the chain length, few types of rotation are physically possible. These are: reorientation of the terminal methyl groups around their C–C bond, either continuously or as a series of 120° jumps between equivalent orientations and the uniaxial rotation of the entire alkyl chain. Each of these predicts a different shape to the EISF that can be used to distinguish between them. As shown **Figure 3(b)**, the model that best fits the data is uniaxial rotation of the entire alkyl chain but with a substantial fraction that is immobile on the instrument's timescale: 82% at 273 K, 71% at 323 K and 64% at 373 K. A temperature-dependant fraction of the oligomers breaks the forces holding them to the pore walls to allow localised rotation. The observation that this motion is free rotation of the alkyl chain around its long axis strongly suggests that the mobile hydrocarbons are located in the straight pore channels in the zeolite.

3.2 Fresh H-ZSM-5 and Propene

Based on the high activity towards low temperature oligomerisation found for 1-octene in ZSM-5-FR, it is to be expected that propene will exhibit similar levels of activity. This is especially true because while previous studies on 1-octene oligomerisation were somewhat ambiguous about the minimum reaction temperature, the literature of propene-zeolite chemistry contains extensive evidence on ZSM-5's capability to catalyse oligomerisation at room temperature or below (20). However, this chemistry provides a route for the generation of C–C bonds and therefore contributes to a number of important chemical processes. For example, light alkene oligomerisation is believed to play an important role in the generation of the 'hydrocarbon pool' in the methanol-to-hydrocarbons reactions (23). They also, as the inverse reaction to the β-scission cracking mechanism, are important contributors to the product stream composition in FCC processes.

Exposure of ZSM-5-FR to propene at room temperature results in the INS spectrum shown in **Figure 4**, Curve A (6). Oligomerisation or polymerisation of propene would be expected to result in a branched alkane or polypropylene. Comparison with spectra of atactic (**Figure 4**, Curve B) and isotactic (**Figure 4**, Curve C) polypropylene shows only poor agreement, comparison with polyethylene (**Figure 4**, Curve D) and the product from 1-octene oligomerisation (**Figure 1(a)**, Curve A) shows that the product is a linear, rather than a branched alkane, hence head-to-tail oligomerisation or polymerisation has occurred.

Unlike 1-octene, it was possible to introduce propene to a sample of ZSM-5-FR without triggering oligomerisation by a modification of the dosing procedure. By cooling the ZSM-5-FR sample cell in liquid nitrogen to the top of the catalyst bed and introducing the propene at the top of the cell, propene was condensed into the sample cell. This was then inserted into the INS spectrometer and heated to 140 K. The propene

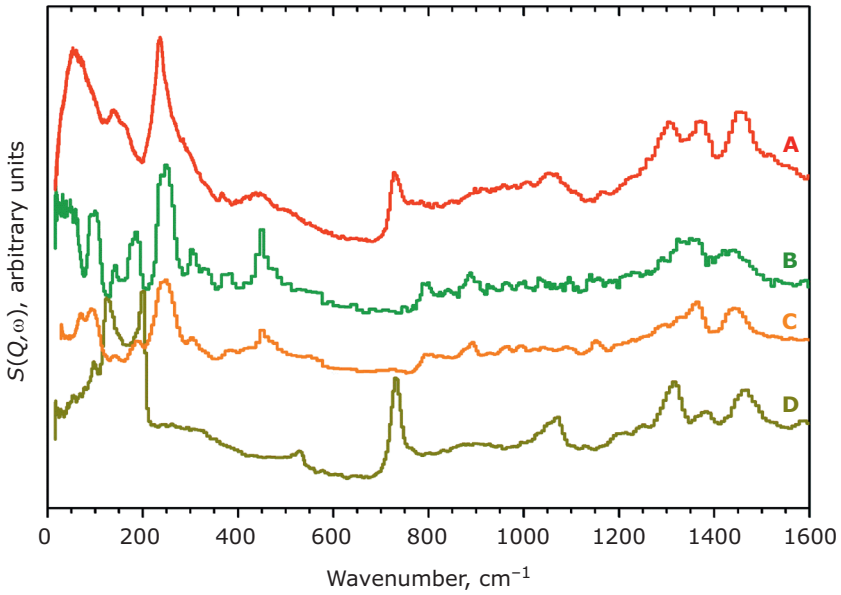

Fig. 4. INS spectrum of propene adsorbed in: A = ZSM-5-FR; compared with reference spectra of: B = atactic polypropene; C = isotactic polypropene; D = polyethylene. Reproduced from (6) under a Creative Commons Attribution (CC-BY) License

 © 2024 Johnson Matthey

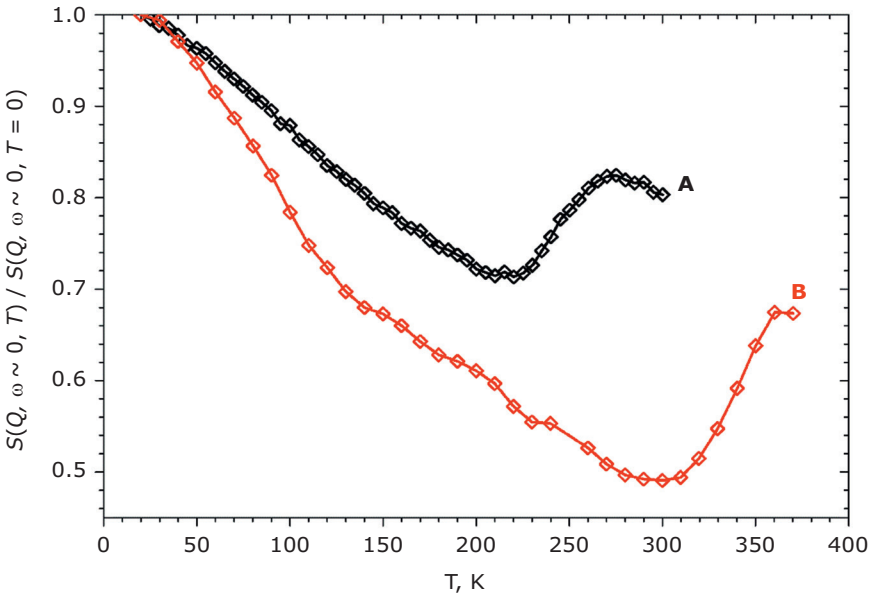

Fig. 5. Elastic fixed window scan data for propene in: A = ZSM-5-FR; B = ZSM-5-ST(873K). Relative elastic intensities normalised against the value at 20 K to allow comparison between samples. Reproduced from (7) under a Creative Commons Attribution 3.0 Unported (CC BY 3.0) licence

melted and diffused into the sample as a liquid. Subsequent cooling of the sample to 10 K and measurement of the spectrum showed that unreacted propene was present and stable within the zeolite.

Since the oligomerisation or polymerisation causes the creation of larger molecules, there is a reduction in the overall mobility of the ZSM-5 or hydrocarbon system as the oligomers molecules are unable to diffuse freely through the zeolite. Hence it was possible to follow the progress of the reaction with temperature by a QENS EFWS analysis as shown in **Figure 5**, Curve A.

Up to 225 K, the EFWS behaves normally and shows the expected decrease in intensity with increasing temperature as the mobility of the propene increases. At 225 K, the intensity increases at the onset of the oligomerisation reaction as propene is converted to less mobile long-chain species. Despite the sample being given time to react and equilibrate at each temperature point, the decrease in mobility is not instantaneous and occurs over the range 225–270 K, in contrast to the rapid and complete oligomerisation at room temperature. Once the oligomerisation is complete, the expected downward trend in elastic intensity with temperature resumes as the products moves more with increasing temperature.

Owing to the physics of INS, specifically the need for low temperature measurements to avoid Debye-Waller effects (12), it is impossible to perform this investigation as a true *operando* measurement. Instead, a stepwise protocol was adopted, where a cryogenically loaded ZSM-5-FR on propene sample was sequentially heated to successively higher temperatures, held for 30 min to allow reaction to occur and then cooled back to ≤30 K to allow spectrum collection. The experiment was performed using TOSCA because detectable changes from the formation of any reaction intermediates are most likely to lie in the C–H deformation region where TOSCA offers better resolution. This analysis was performed across the temperature range of interest identified by the QENS analysis above, giving the spectra in **Figure 6**.

Examination of the post-140 K INS spectrum (**Figure 6**, Curve A) shows all the modes of pure propene are present, confirming that the propene adsorption process has been completed successfully without oligomerisation. A close examination of the spectrum does show one difference from the free propene data: the =C–CH_3 torsional mode at 221 cm^{-1} splits to a complex feature with peaks at 200 cm^{-1}, 216 cm^{-1} and 230 cm^{-1}.The presence of three peaks in the 140 K spectrum, shows that the propene is present in multiple environments in this sample, possibly representing internally and externally adsorbed propene. Above 250 cm^{-1} differences between the free and 140 K adsorbed propene spectra are minor. Besides the methyl torsion, modes of interest are the vinyl scissors mode at 429 cm^{-1} (§) and the vinyl torsion at 584 cm^{-1} (†).

After heating the sample to 200 K (**Figure 6**, Curve B) some changes are apparent, even though the QENS data shows that this temperature is below the point at which changes in sample mobility begin. Notably, the 585 cm^{-1} peak, (the twisting motion

 © 2024 Johnson Matthey

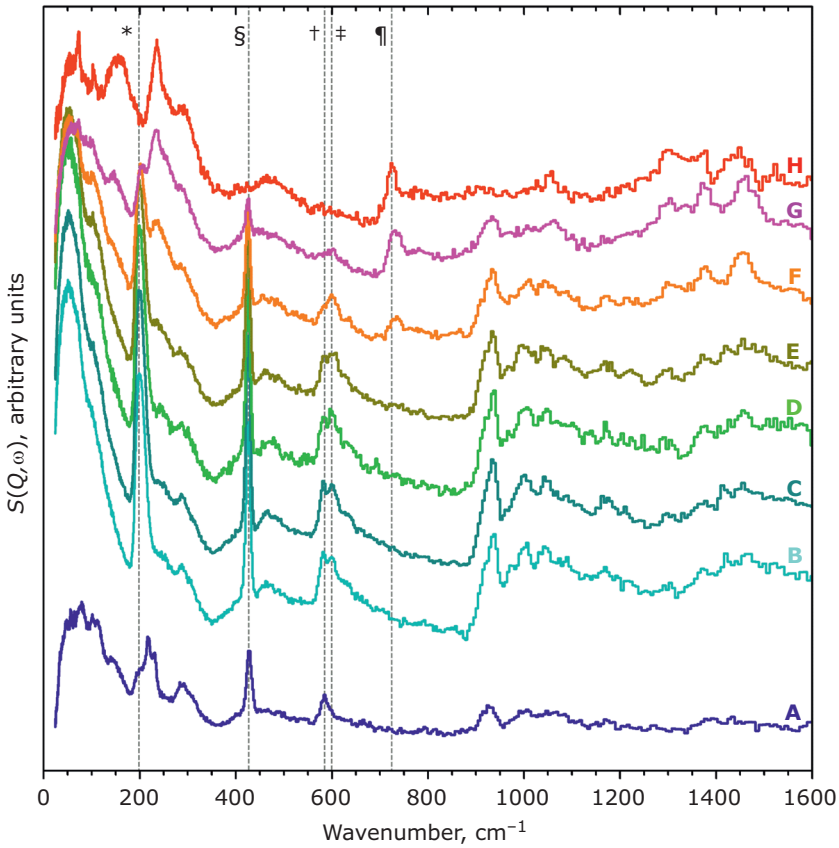

Fig. 6. INS spectra recorded on TOSCA of propene: A = after absorption into ZSM-5-FR at 140 K; then following further heating to: B = 200 K; C = 215 K; D = 225 K; E = 240 K; F = 255 K; G = 270 K and H = 293 K. All spectra were recorded below 20 K. Spectra are *y*-offset for clarity. The positions of the methyl torsion (*), vinyl scissors (§) and non-bonded and bonded vinyl torsions (†, ‡) in the 200 K spectrum and the in-phase methylene rock (¶) in the final oligomer spectrum are highlighted. Adapted from (6) under a Creative Commons Attribution 4.0 International license (CC-BY)

about the propene C=C bond), splits into two peaks at 581 cm^{-1} (†) and 600 cm^{-1} (‡). This is assigned to the formation of propene hydrogen-bonded to a Brønsted acid site through the π orbitals of the C=C double bond. This intermediate is assigned to the higher energy peak in the doublet and the remaining physisorbed propene to the 581 cm^{-1} band. The formation of hydrogen-bonded intermediates as the first step in the oligomerisation reactions of light alkenes over acid zeolites is known (17). Although the H-bonded intermediates are only observed experimentally here at low temperature, this is regarded as a spectroscopic limitation owing to their transience at higher temperatures. Computational studies agree that H-bonded π-complexes are a necessary first intermediate in the oligomerisation at temperatures closer to industrial conditions (20).

An increase in overall spectral intensity relative to the spectrum post-140 K is seen (*c.f.* **Figure 6**, Curves A and B), consistent with an increase in the amount of hydrogen in the neutron beam. Since the sample cell is a closed system, the most likely source of the additional hydrogen is from the adsorption of propene previously located in the headspace of the sample cell into the zeolite. No further intensity increases are seen for the subsequent temperatures, showing that all the propene is adsorbed at 200 K and above. This is supported by the shift of all the methyl torsion intensity into a single peak at 200 cm^{-1} (*), indicating that all the propene present is now in the same environment and that the 200 cm^{-1} peak in the 140 K spectrum represents the fraction of the propene which is within the zeolite pore network at that temperature. Since neither the methyl torsion (*) nor the vinyl $=CH_2$ scissors modes (§) are split, the hydrogen bonding in the intermediate is not strong enough to modify modes that do not involve the C=C bond itself.

Further heating to 215 K (**Figure 6**, Curve C) and 225 K **Figure 6**, Curve D does not result in significant changes, although some transfer of intensity occurs between the 581 cm^{-1} and 600 cm^{-1} peaks, indicating a slight increase in the proportion of hydrogen-bonded propene. At 240 K (**Figure 6**, Curve E) there are new changes: a reduction in the intensity of peaks associated with the vinyl group, most clearly seen in the vinyl scissors mode at 430 cm^{-1} (§) and a new peak begins to grow in at 235 cm^{-1}, which is a more typical value for methyl torsions in a long chain alkane (21).

At 255 K (**Figure 6**, Curve F) a broad longitudinal acoustic mode of the oligomer becomes apparent above the background noise at 155 cm^{-1}. At

© 2024 Johnson Matthey

this temperature there is a further reaction step which consumes the C=C bond, as evidenced by reductions in the intensities of the vinyl modes (§, †, ‡), and leads to the formation of methylene modes, particularly the in-phase rock at 728 cm^{-1} (¶). This confirms the initiation of the oligomerisation reaction step; taking difference spectra of the higher temperature data highlights these changes and indicates that the oligomerisation has actually begun by 240 K. The growth of methylene peaks (¶ and the 1300–1500 cm^{-1} region) continues up to the highest temperature measured (293 K). Some propene molecules remain at temperatures as high as 270 K, although at this temperature the 581 cm^{-1} peak has been completely suppressed, so the propene is purely present in the hydrogen-bonded form.

3.3 Steam Dealuminated H-ZSM-5 and Propene

The mean diffusion path and the acid site density within a zeolite are important factors in determining how it interacts with guests and hence its activity. However, the acid properties are not constant throughout the catalyst's useful lifetime, as the hydrothermal conditions typically found in catalytic use result in partial dealumination of the zeolite framework. There is a corresponding reduction in the number of acid sites and some increased mesoporosity due to removal of part of the framework (21).

To investigate the effects of acid site loss, partially dealuminated zeolite samples were prepared in order to compare their properties with the results obtained from investigations of ZSM-5-FR. Since the rate of the dealumination is first order in aluminium (22), this means that the catalyst will spend the majority of its catalytic lifetime in a significantly dealuminated state, hence the steam treatment conditions were deliberately chosen in order to induce a high level of acid site loss. This was successful: steaming at 873 K resulted in ~95% loss of Brønsted sites and the silanols (this catalyst is designated as ZSM-5-ST(873)). Other physical properties of the material including surface area, micropore and mesopore volume and the X-ray diffraction pattern were largely unchanged (7).

Figure 5, Curve B shows the EFWS for propene in the dealuminated sample, ZSM-5-ST(873). It is apparent that the oligomerisation requires higher temperatures for initiation. The first indication of oligomerisation is at 290 K as the elastic window trace deviates from the linear decrease with temperature observed from 130–280 K. Propene persists to much higher temperatures as the EFWS does not turn over until 360 K, in the case of ZSM-5-FR, the reaction is complete by 300 K. Besides decreased reactivity, the EFWS plot dramatically demonstrates the effect of the steam treatment on the overall mobility of the propene within the zeolite. Strikingly, the ZSM-5-ST(873 K) sample shows much higher mobility below 200 K, where there is no oligomerisation in either sample. The difference is caused by a more rapid increase in mobility in ZSM-5-ST(873 K) from 20–140 K. Above 140 K, there is a visible inflection in the **Figure 5**, Curve B trace, above which the rate of mobility increase in both samples appears similar.

The linear nature of the ZSM-5-ST elastic window plot from 130–280 K suggests that the adsorbed propene is undergoing similar motions across this range and allows us to characterise these motions in more detail by high SNR spectra collected at 170 K, 220 K and 270 K. All spectra required the inclusion of a linear background, in addition to the resolution function. In fitting the 220 K and 270 K spectra, the remaining quasielastic component was described by a single Lorentzian, corresponding to a single motion occurring within the instrument's time window. For the 170 K dataset, this model did not produce an acceptable fit to the data and better results were obtained by use of two Lorentzian functions. One of these had similar *Q*-dependant behaviour to that observed at higher temperatures and the second was considerably broader.

For the Lorentzian that is observed at all temperatures, the variation of its half width at half maximum as a function of Q^2 (**Figure 7(a)**) displays similar behaviour at all three temperatures. Fitting the data to the Singwi-Sjölander jump diffusion model gives the fits shown by the dotted lines in **Figure 7(a)**. The Singwi-Sjölander model assumes a molecule resides on a lattice point for a fixed time and then executes jumps with a distribution of distances. The root mean square jump distance is ~2.8 Å. This indicates that the jumps are not occurring between pore intersections in the zeolite framework, these are separated by 9 Å in the straight [010] channels and 12 Å in the [100] channels but is movement on a shorter length scale. Since the distance is also less than the diameter of the 10-ring framework window (5.1 × 5.5 Å in the narrower sinusoidal channel) it is likely that propene-propene interactions play a major role in determining the favoured jump length.

The second Lorentzian (see **Figure 7(b)**) is only observed at 170 K and is considerably broader (compare the y-axes in **Figure 7(a)** and **7(b)**).

© 2024 Johnson Matthey

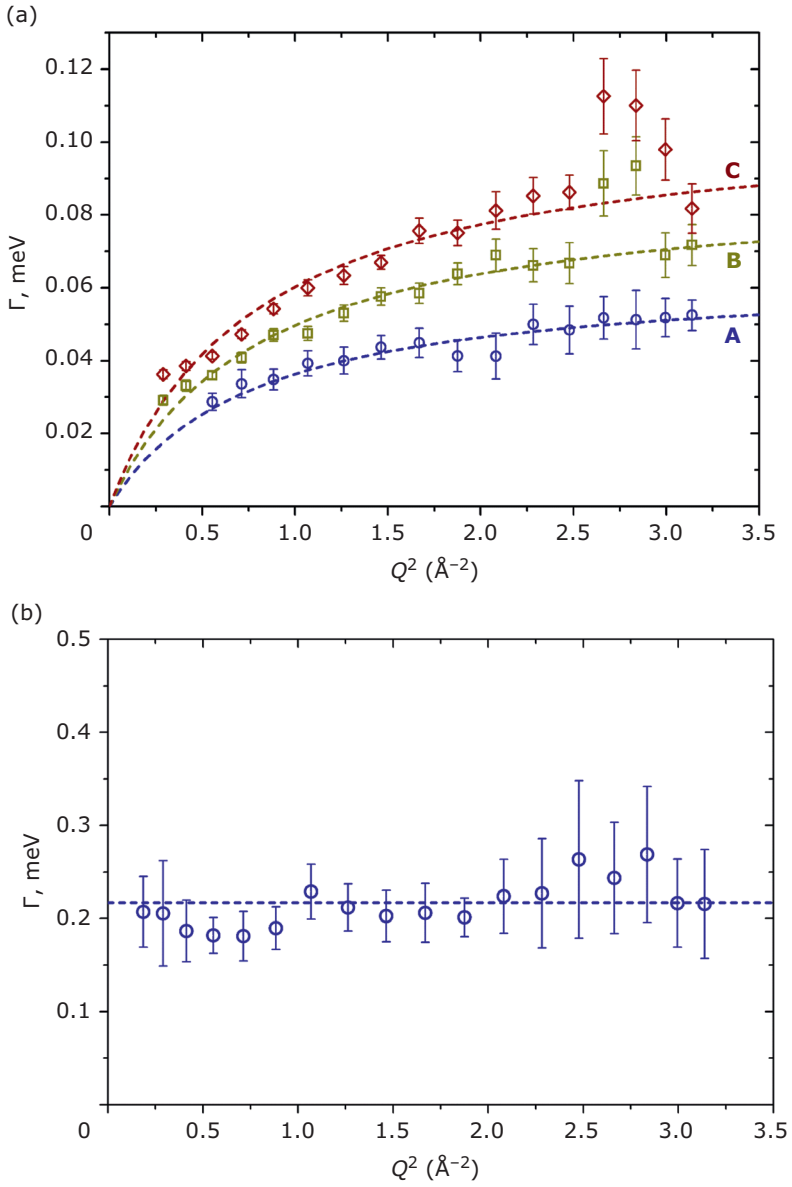

Fig. 7. (a) Variation of the Lorentzian linewidth (Γ) as a function of Q^2 for propene in ZSM-5-ST(873K) for: A = 170 K; B = 220 K; C = 270 K. Dotted lines are the best fit to the Singwi-Sjölander model of jump diffusion; (b) the second Lorentzian observed for propene in ZSM-5ST(873K) at 170 K showing *Q*-independent behaviour. Dotted line represents the best fit. Reproduced from (7) under a Creative Commons Attribution 4.0 International license (CC-BY)

Within the limits of experimental accuracy, the *Γ* values are constant and independent of *Q*, showing that this corresponds to a rotational movement of the propene. The best fit to the experimental values shows the rotational constant for the motion to be D_r = 3.29 × 10^{11} s^{-1}. The absence of this Lorentzian at higher temperatures, indicates that it represents a rapid rotation of the propene molecule that is only observable at extremely low energies. At higher temperatures the propene moves quickly enough that it is outside the instrument's time window, so merges into the flat background. This motion has not been reported previously because the measurements are generally performed at higher temperatures.

Loading propene into ZSM-5-ST(873K) at low temperature and measuring the spectra as a function of reaction temperature, as done in **Figure 6**, produces the spectra shown in **Figure 8**.

The spectra confirm the QENS results. The first unambiguous sign of oligomerisation is not seen until 290 K, when the in-phase rock mode (dashed line and ‡) of the oligomer at ~720 cm^{-1} rises above the background (**Figure 8**, Curve E).

© 2024 Johnson Matthey

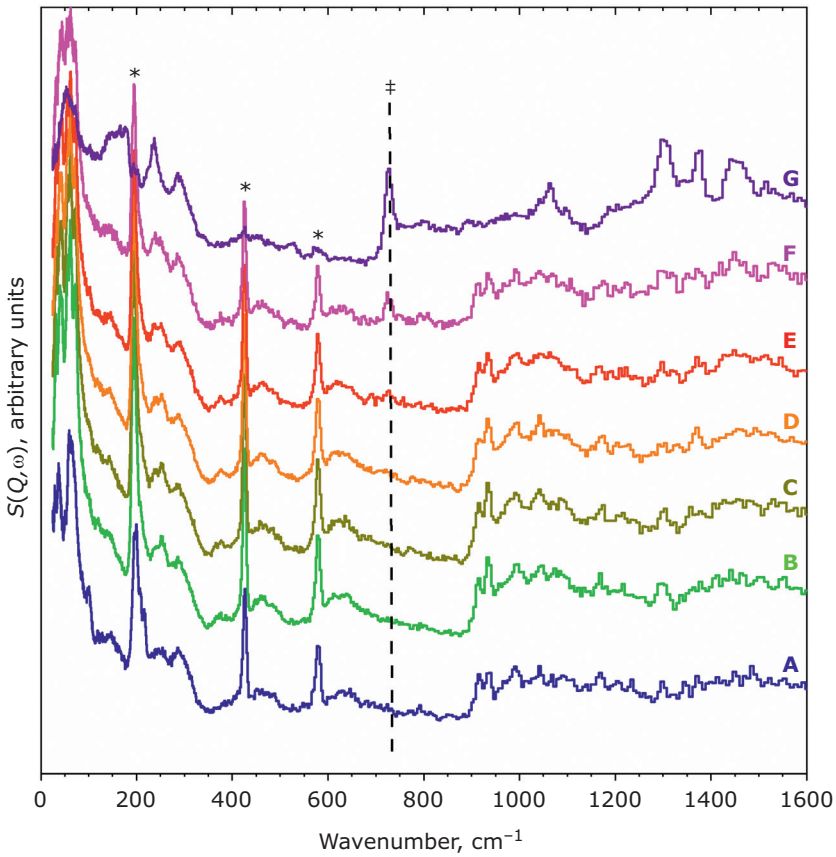

Fig. 8. TOSCA INS spectra of propene: A = after absorption into ZSM-5ST(873K) at 140 K; then following further heating to the indicated temperatures: B = 260 K; C = 270 K; D = 280 K; E = 290 K; F = 300 K; G = 325 K. Spectra are offset in the *y*-axis for clarity. The 720 cm^{-1} oligomer rock band is marked by a dashed line and ‡. The major propene bands are indicated by *. Adapted from (7) under a Creative Commons Attribution 3.0 Unported (CC BY 3.0)

The small quantity of unreacted propene (*) in **Figure 8**, Curve G suggests that the reaction does not proceed to completion even at 325 K, which was the highest temperature investigated by INS. The reduced acidity of ZSM-5ST(873K) means that a higher temperature is required to initiate the propene protonation. This is believed to be the rate-limiting step in the oligomerisation reaction.

With the steamed catalyst, the formation of the hydrogen bonded propene intermediate and associated splitting of the propene vinyl torsion peak is not seen. As the mechanism of the oligomerisation in unlikely to have changed, the reduced number of acid sites means that the population of hydrogen-bonded propene in ZSM-5-ST(873K) is below the INS detection limit, even when all the acid sites are occupied. The difference in behaviour between the fresh and steamed zeolites results in slight differences in the composition of the resulting oligomer. Although in both cases the final product spectrum is characteristic of a primarily linear series of oligomer chains, the spectra have different relative peak intensities. In particular, the relative intensity of the methyl torsion has deceased while the in-phase methylene rock in the ZSM-5-ST(873K) oligomer spectrum has, relatively, increased. This is consistent with both a greater average chain length than in ZSM-5-FR and our suggestion that the average oligomer chain length is determined by steric effects causing termination of chain formation. One end of the oligomer is fixed at the catalytic site by protonation while the other end of the molecule grows through the pore network as the chain is extended by further addition of propene. For the majority of oligomers at interior sites, the maximum length limitation will be when this end of the chain encounters a pore channel that is already occupied by another chain, preventing further growth. Since ZSM-5-ST(873K) has fewer, more widely spaced active sites, longer oligomers can be accommodated further before they intersect another oligomer and are blocked, resulting in the observed increase in average chain length.

4. Conclusions

INS and QENS have been applied to the study of the reactivity of alkenes over the acid zeolite catalyst H-ZSM-5. Both techniques provide new insights into the reaction chemistry and dynamics which

 © 2024 Johnson Matthey

occur inside zeolites and exhibit a clear synergy when employed in combination. The INS results provide information on the interactions responsible for changes in mobility and broad-range QENS results, collected through the EFWS method, guiding the assignment of INS measurements to the temperatures of greatest interest.

Investigation of the interactions of alkenes in fresh H-ZSM-5 have shown that the extremely high activity of the catalyst causes the alkenes to undergo protonation and subsequent oligomerisation even at low temperatures, with reactivity for propene commencing at 225 K. Examination of the reaction intermediates by INS, shows that the first step is the formation of hydrogen-bonded intermediate and that the subsequent protonation of the alkene to a bonded carbocation represents the rate-limiting stage of the reaction. Examination of the product spectra suggests, that for both propene and 1-octene, pore wall interactions result in reactions at interior acid sites producing linear oligomers which form the bulk of the final product.

This oligomerisation activity prevents the measurement of the movement of propene or 1-octene in fresh zeolites by QENS. It is possible to observe the movement of the oligomers themselves, which are trapped within the pore network, and are capable of rotating around their long axis within the straight channels of the zeolite. Studies using propane as an inert analogue for propene have found, in concert with molecular dynamics simulations, that the adsorbed C3 molecules spend the majority of their time undergoing short jumps within the pore channels of the zeolite (24). Movement into the pore intersections is disfavoured and longer-range diffusion takes place by longer jumps across the pore channels at intervals too long to be observed by the QENS instruments employed.

Hydrothermal dealumination plays an important role in determining the activity of zeolite catalysts and occurs rapidly enough in industrial use that studies using fresh materials do not accurately represent the zeolite's activity for the majority of its catalytic lifetime. At low temperatures for hydrocarbon reaction, this dealumination was found to have the effect of delaying the onset of catalytic activity for oligomerisation to higher temperatures and increasing the mobility of hydrocarbons within the zeolite, both due to reduced acid-hydrocarbon interactions. The mobility increase was not found to result from changes in the geometry of the molecular motions, but purely due to them occurring at shorter intervals, indicating that this geometry is defined by structural factors arising from the framework itself, rather than the acid sites.

Neutron techniques have proven to be powerful tools for the analysis of catalytic reactivity of hydrogenous materials in zeolite catalysts. The potential for applying these methods to other questions involving zeolite catalytic chemistry is clear.

Acknowledgements

Johnson Matthey plc is thanked for supplying the ZSM-5 zeolite and for financial support through the provision of industrial CASE studentships in partnership with the EPSRC (APH (EP/P510506/1, AZ (EP/N509176/1)). The resources and support provided by the UK Catalysis Hub *via* membership of the UK Catalysis Hub consortium and funded by EPSRC grants EP/R026815/1 and EP/R026939/1 are gratefully acknowledged. This research has been performed with the use of facilities and equipment at the Research Complex at Harwell; the authors are grateful to the Research Complex for this access and support. The ISIS Neutron and Muon Facility is thanked for access to neutron beam facilities (25–31).

References

1. R. J. Argauer, M. G. R. Landolt, Mobil Oil Corp, 'Crystalline Zeolite ZSM-5 and Method of Preparing the Same', *US Patent* 3,702,886; 1972
2. 'Database of Zeolite Structures', International Zeolite Association, 2017
3. A. Corma, *Chem. Rev.*, 1995, **95**, (3), 559
4. A. P. Hawkins, A. J. O'Malley, A. Zachariou, P. Collier, R. A. Ewings, I. P. Silverwood, R. F. Howe, S. F. Parker, D. Lennon, *J. Phys. Chem. C*, 2018, **123**, (1), 417
5. A. P. Hawkins, A. Zachariou, P. Collier, R. A. Ewings, R. F. Howe, S. F. Parker, D. Lennon, *RSC Adv.*, 2019, **9**, (33), 18785
6. A. P. Hawkins, A. Zachariou, S. F. Parker, P. Collier, I. P. Silverwood, R. F. Howe, D. Lennon, *ACS Omega*, 2020, **5**, (14), 7762
7. A. P. Hawkins, A. Zachariou, S. F. Parker, P. Collier, N. Barrow, I. P. Silverwood, R. F. Howe, D. Lennon, *RSC Adv.*, 2020, **10**, (39), 23136
8. A. P. Hawkins, A. Zachariou, S. F. Parker, P. Collier, R. F. Howe, D. Lennon, *Catal. Sci. Technol.*, 2021, **11**, (8), 2924
9. A. T. Boothroyd, "Principles of Neutron Scattering from Condensed Matter", Oxford University Press,

 © 2024 Johnson Matthey

Oxford, UK, 2020

10. M. T. F. Telling, "A Practical Guide to Quasi-elastic Neutron Scattering", Royal Society of Chemistry, Cambridge, UK, 2020, 152 pp
11. P. C. H. Mitchell, S. F. Parker, A. J. Ramirez-Cuesta, J. Tomkinson, "Vibrational Spectroscopy with Neutrons: With Applications in Chemistry, Biology, Materials Science and Catalysis", Series on Neutron Techniques and Applications, Vol. 3, World Scientific Publishing Co Pte Ltd, Singapore, 2005
12. S. F. Parker, P. Collier, *Johnson Matthey Technol. Rev.*, 2016, **60**, (2), 132
13. F. Polo-Garzon, S. Luo, Y. Cheng, K. L. Page, A. J. Ramirez-Cuesta, P. F. Britt, Z. Wu, *ChemSusChem*, 2018, **12**, (1), 93
14. X. Yu, Y. Cheng, Y. Li, F. Polo-Garzon, J. Liu, E. Mamontov, M. Li, D. Lennon, S. F. Parker, A. J. Ramirez-Cuesta, Z. Wu, *Chem. Rev.*, 2023, **123**, (13), 8638
15. A. Zachariou, A. P. Hawkins, R. F. Howe, J. M. S. Skakle, N. Barrow, P. Collier, D. W. Nye, R. I. Smith, G. B. G. Stenning, S. F. Parker, D. Lennon, *ACS Phys. Chem. Au*, 2023, **3**, (1), 74
16. A. Zachariou, A. P. Hawkins, P. Collier, R. F. Howe, S. F. Parker, D. Lennon, *Catal. Sci. Technol.*, 2023, **13**, (7), 1976
17. J. R. Anderson, Y.-F. Chang, R. J. Western, *Appl. Catal.*, 1991, **75**, (1), 87
18. 'ISIS Neutron and Muon Source', Science and Technology Facilities Council, Swindon, UK: https://www.isis.stfc.ac.uk/Pages/About.aspx (Accessed on 1st March 2024)
19. S. F. Parker, D. Lennon, P. W. Albers, *Appl. Spectrosc.*, 2011, **65**, (12), 1325
20. G. Spoto, S. Bordiga, G. Ricchiardi, D. Scarano, A. Zecchina, E. Borello, *J. Chem. Soc., Faraday Trans.*, 1994, **90**, (18), 2827
21. J. Tomkinson, S. F. Parker, D. A. Braden, B. S. Hudson, *Phys. Chem. Chem. Phys.*, 2002, **4**, (5), 716
22. A. G. Stepanov, M. V. Luzgin, V. N. Romannikov, K. I. Zamaraev, *Catal. Lett.*, 1994, **24**, (3–4), 271
23. U. Olsbye, S. Svelle, K. P. Lillerud, Z. H. Wei, Y. Y. Chen, J. F. Li, J. G. Wang, W. B. Fan, *Chem. Soc. Rev.*, 2015, **44**, (20), 7155
24. A. P. Hawkins, 'The Application of Neutron Scattering to Investigate Hydrocarbon Conversion over Zeolite Catalysts', PhD Thesis, School of Chemistry, College of Science and Engineering, University of Glasgow, UK, June, 2021, 355 pp
25. D. Lennon, S. Matam, R. Howe, I. Hitchcock, S. Parker, A. York, P. Collier, A. Hawkins, A. Zachariou, 'Studies of Propene Formation by gasoline Cracking in Steamed ZSM-5 by INS', Experiment No. RB1620408, ISIS Neutron and Muon Source Data, Science and Technology Facilities Council, Swindon, UK, 2016
26. D. Lennon, P. Collier, A. Hawkins, S. Parker, A. Zachariou, 'INS studies of the interaction of propene with ZSM-5', Experiment No. RB1720047, ISIS Neutron and Muon Source Data, Science and Technology Facilities Council, Swindon, UK, 2017
27. D. Lennon, P. Collier, A. Hawkins, S. Parker, A. Zachariou, 'Studies of the Effect of Steaming on Catalyst-Substrate Interactions in ZSM-5 Cracking Catalysts', Experiment No. RB1810123, ISIS Neutron and Muon Source Data, Science and Technology Facilities Council, Swindon, UK, 2017
28. D. Lennon, A. Hawkins, P. Collier, S. Parker, I. Silverwood, A. Zachariou, 'QENS Studies of the Interaction of Propene with ZSM-5', ISIS Experiment No. RB1720048, ISIS Neutron and Muon Source Data, Science and Technology Facilities, Council, Swindon, UK, 2018
29. D. Lennon, A. Zachariou, P. Collier, A. Hawkins, S. Parker, 'Studies of Catalyst-Substrate Interactions in an Industrial ZSM-5 Cracking Catalyst', ISIS Experiment No. RB1820118, ISIS Neutron and Muon Source Data, Science and Technology Facilities Council, Swindon, UK, 2018
30. D. Lennon, A. Zachariou, P. Collier, I. P. Silverwood, A. Hawkins, S. Parker, 'Diffusion of Model Hydrocarbon Species in a Steady-State Industrial Zeolite Cracking Catalyst', ISIS Experiment No RB1820119, ISIS Neutron and Muon Source Data, Science and Technology Facilities Council, Swindon, UK, 2018
31. R. Howe, Y. Li, S. Huang, I. Hitchcock, D. Lennon, S. Parker, A. Hawkins, A. Zachariou, 'INS Studies of Olefin Reactivity in HZSM-5 Zeolite Catalysts', ISIS Experiment No RB1910203, ISIS Neutron and Muon Source Data, Science and Technology Facilities Council, Swindon, UK, 2019

 © 2024 Johnson Matthey

The Authors

Alexander P. Hawkins is a postdoctoral researcher at the UK Central Laser Facility (CLF). After working in the fuel cells division of Johnson Matthey he undertook his PhD research in neutron scattering studies of hydrocarbon conversions at the University of Glasgow, UK. He subsequently moved to the CLF under Paul Donaldson, using ultrafast vibrational IR spectroscopy to study zeolite-catalysed reactions and adsorbate dynamics.

Andrea Zachariou earned her PhD at the University of Glasgow in 2021, supervised by Professor David Lennon and Professor Stewart Parker. The PhD was industrially sponsored by Johnson Matthey and focused on using neutron spectroscopic techniques in combination with other analytical techniques to study heterogeneous catalysts, with a focus on the ZSM-5 catalyst used for the MTH reaction. For the duration of the PhD, Andrea was based at the UK Catalysis Hub at the Research Complex in Harwell. In 2021 she went on to join the group of Simon K. Beaumont in Durham University, UK.

Paul Collier is a Research Fellow at Johnson Matthey, Sonning Common, UK. He is responsible for organising Johnson Matthey's collaborations at the Harwell site, 25 km from Johnson Matthey's site at Sonning Common, which hosts the world class facilities such as the UK's synchrotron (Diamond) and the ISIS neutron spallation source. He is interested in heterogeneous and homogeneous catalysis, MOFs, platinum group metals, oxidation, synchrotron, neutron diffraction, neutron spectroscopy, lasers, zeolite catalysts, methane and alkanes.

Russell Howe is an Emeritus Professor of Materials Chemistry at the University of Aberdeen. Following education in New Zealand he pursued postdoctoral studies at Edinburgh University, Texas A and M and CSIRO Australia before taking academic positions at the University of Wisconsin-Milwaukee, University of Auckland, University of New South Wales and University of Aberdeen, UK (since 2001). His interests are in applications of spectroscopy to study materials, surfaces and catalysts

David Lennon is Professor of Physical Chemistry at the University of Glasgow, UK where he heads the Heterogeneous Catalysis Section. He has approximately 30 years' experience of applying neutron scattering techniques (mainly INS) to examine chemistry at the gas/solid interface. A significant body of that work has been undertaken in partnership with industry. In 2021 DL was awarded the STFC ISIS Facility Impact Award – Economy.

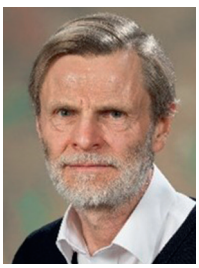

Stewart F. Parker is the ISIS Catalysis Scientist. After earning his PhD at the University of California at Santa Barbara, USA, he moved to the University of East Anglia under Professor Mike Chesters to apply Fourier transform infrared spectroscopy to adsorbates on metal single crystals. He then joined the BP Research Centre at Sunbury-on-Thames working in the Analytical Division on infrared spectroscopy of polymers and catalysts. In 1993 he joined ISIS as an instrument scientist. His interests are the application of vibrational spectroscopy and neutron scattering to investigate chemical problems, especially in catalysis.

© 2024 Johnson Matthey